




Aluminum-induced high IAA concentration may explain the Al susceptibility in *Citrus limonia*

Carolina M. S. Silva¹ · Mariana F. Cavaleiro¹ · Anna C. G. Bressan¹ · Brenda M. O. Carvalho¹ · Otavia F. A. A. Banhos¹ · Eduardo Purgatto² · Ricardo Harakava³ · Francisco A. O. Tanaka⁴ · Gustavo Habermann⁵ 

Received: 22 January 2018 / Accepted: 15 November 2018 / Published online: 22 November 2018
© Springer Nature B.V. 2018

Abstract

In acidic soils (pH < 5.0), aluminum (Al) occurs as Al³⁺, which is phytotoxic and reduces the root growth by hormonal imbalance and/or cell wall rigidity. However, the explanations for the decrease in root growth are not clear. A 60-day study was held with ‘Rangpur’ lime (*Citrus limonia*) plants grown in nutrient solution containing 0 and 1480 μM Al. We measured plant biometric data and used root apices to analyze auxin (IAA), the expression of some Al-responsive genes that had been differentially expressed in a transcriptome analysis and anatomical profiles. We found up-regulated expression of multidrug and toxic compound exudation (*Cl-MATE* channel), citrate synthase (*Cl-CS*) and pectin methylesterase inhibitor (*Cl-PMEI*) genes, but while *Cl-PMEI* expression was increased after 7 days, *Cl-CS* and *Cl-MATE* were up-regulated only after 60 days, suggesting that the timing of these events was ineffective against Al. These results could be associated with the Al-induced decrease in root growth and anatomical root damage. In addition, genes related to IAA cell transport were not differentially expressed in the transcriptome analysis. Therefore, high IAA and up-regulation of auxin-related small RNAs suggest Al-induced high IAA concentration rather than Al-induced disruption in IAA distribution in root cells of this species.

Keywords Al³⁺ · Auxin · Efflux channels · Gene expression · ‘Rangpur’ lime · Root growth

Introduction

Aluminum (Al) is the third most abundant element in the Earth’s crust and, in the soil, it naturally occurs as Al₃SiO₄ (Von Uexküll and Mutert 1995). Approximately 30–45% of soils from the world’s ice-free land are acidic (pH < 5.0) (Von Uexküll and Mutert 1995) and, under this condition

Al₃SiO₄ is hydrolyzed to Al³⁺, which is toxic to most plants (Kochian 1995). In plants that are sensitive to Al, it is covalently retained in the apoplast of root cells showing direct effects such as inhibition of root growth (Kochian 1995; Horst et al. 2010; Sun et al. 2010), which is one of the most conspicuous symptoms of Al toxicity. It can also have indirect effects reducing shoot growth (Jiang et al. 2008) and leaf gas exchange (Chen et al. 2005; Banhos et al. 2016).

In plants not exposed to Al, ethylene upregulates auxin biosynthesis to inhibit root cell elongation (Swarup et al. 2007), a known crosstalk between ethylene and auxin for

Electronic supplementary material The online version of this article (<https://doi.org/10.1007/s10725-018-0458-5>) contains supplementary material, which is available to authorized users.

✉ Gustavo Habermann
gustavo.habermann@unesp.br

¹ Programa de Pós-Graduação em Ciências Biológicas (Biologia Vegetal), Instituto de Biociências, Departamento de Botânica, Universidade Estadual Paulista, UNESP, Av. 24-A, 1515, Rio Claro, SP 13506-900, Brazil

² Departamento de Alimentos e Nutrição Experimental/NAPAN/FoRC-Food Research Center, Faculdade de Ciências Farmacêuticas, Universidade de São Paulo, USP, Av. Prof. Lineu Prestes, 580, bl 14, São Paulo, SP 05508-000, Brazil

³ Centro de P&D de Sanidade Vegetal, Laboratório de Bioquímica Fitopatológica, Instituto Biológico, Av. Conselheiro R. Alves, 1252, São Paulo, SP 04014-002, Brazil

⁴ Departamento de Fitopatologia e Nematologia, Escola Superior de Agricultura “Luiz de Queiróz” - Universidade de São Paulo, ESALQ-USP, Av. Pádua Dias, 11, Piracicaba, SP 13418-900, Brazil

⁵ Departamento de Botânica, Instituto de Biociências, Universidade Estadual Paulista, UNESP, Av. 24-A, 1515, Rio Claro, SP 13506-900, Brazil

proper root growth. In plants exposed to Al, the toxicity perception was evidenced to occur at the root apex of maize (*Zea mays*) (Ryan et al. 1993), and the ethylene/auxin crosstalk seems to be affected. In fact, Al-induced ethylene biosynthesis could act as a signal to modify auxin distribution in roots of *Arabidopsis thaliana* by disrupting genes encoding proteins for polar transport of auxin, such as *At-AUX1* and *At-PIN2*, which eventually leads to arrest of root elongation (Sun et al. 2010). Al-induced increase in auxin biosynthesis could also lead to inhibition of cell elongation because, in roots, the high concentration of auxin can cause inhibition of cell elongation (Ryan et al. 1993; Rahman et al. 2007). For instance, an Al-induced increased biosynthesis of indole-acetic acid (IAA) was found in the root apex of *Arabidopsis* (Yang et al. 2014).

Al toxicity has been demonstrated not only in *Arabidopsis* and maize, but also in woody species, like *Citrus* plants, where these mechanisms are still unclear. *Citrus limonia* L. (Rutaceae) ('Rangpur' lime) shows reduced root length after being exposed to 400 μM Al for 70 days (Pereira et al. 2003). This species shows significant drought resistance due to a vigorous root system, being important as rootstock in subtropical regions of the Americas (Ribeiro and Machado 2007). Thus, Al-induced decrease in root length has a tremendous impact on this species.

In a range of Al-tolerant species, including herbaceous crop plants (Ryan et al. 2011) and woody species (Brunner and Sperisen 2013), a mechanism to cope with Al involves the efflux of organic anions (malate, citrate, oxalate and succinate), which chelate the toxic Al form (Al^{3+}) preventing its absorption or binding to the cell wall. Malate efflux is mediated by the ALMT channel—aluminum activated malate transporter (Sasaki et al. 2004), and a non-specific protein that belongs to the MATE family (multidrug and toxic compound exudation) operates citrate efflux (Magalhaes 2010). Considering organic acid secretion, two patterns are evident depending on Al response: no delayed response that corresponds to channel activation (pattern I) and response in a lag phase (pattern II), which involves gene expression activation (Ma 2000). In *Citrus grandis* and *C. sinensis*, the secretion of citrate and malate from excised roots exposed to Al was noted within hours, suggesting pattern I response in these species (Yang et al. 2011), but excised roots do not maintain normal metabolic activities for a long time as occurs in vivo. In addition, to our knowledge, no gene expression of secretion channels has been evidenced in order to support Al susceptibility in *Citrus* plants.

Another mechanism to cope with Al relies on cell wall composition, which can interfere with Al affinity. In the absence of Al, the action of pectin methylesterase (PME) leads to free pectic carboxylic groups, allowing the normal cell elongation; in the presence of Al, however, it covalently binds to pectic nets in the cell wall (Horst et al. 2010), which

becomes rigid and limits cell elongation (Kopittke et al. 2008; Blamey et al. 2011). Therefore, the pectin methyl-esterase inhibitor (PMEI) enzyme impedes PME action and could decrease Al binding in the cell wall and, consequently, enhance Al resistance (Schmohl et al. 2000). The secretion of Al-organic acid complexes, enzymatic protection of pectic carboxylic groups in the cell wall, as well as IAA biosynthesis is well documented. However, the measurement of these parameters in whole plants with their entire root system exposed to Al for several days is lacking in the literature.

In a 60-day study, we grew young 'Rangpur' lime plants in a hydroponic system in the presence and absence of Al. We confirmed that Al decreases the root growth in this species, and also performed a transcriptome analysis, in which we expected to find differentially expressed genes related to the secretion of organic acid-Al complexes. We also evidenced the biosynthesis and secretion of organic acids from roots of whole plants. Although expecting to find changes in gene expression of MATE and ALMT gene families, as evidenced by citrate and malate secretion in *Citrus grandis* and *C. sinensis* (Yang et al. 2011), we hypothesized that the expression of these genes is not consistent over time of Al exposure because 'Rangpur' lime plants are known to be sensitive to Al (Pereira et al. 2003; Banhos et al. 2016). We collected root tips and measured IAA which, along with IAA polar transport genes possibly evidenced by the transcriptome and further gene expression analyses, made us predict that IAA distribution in root cells is also disrupted, as shown for *Arabidopsis* (Sun et al. 2010). In addition, anatomical investigation of roots provided evidence to support the functional analyses.

Material and methods

Plant material and experimental conditions

We used 3 month-old and 7 ± 0.5 cm-high 'Rangpur' lime (*C. limonia* L.) plants, showing approximately five leaves, for studying the effects of Al on root development within a 60-day period. The plants were grown directly on an aerated nutrient solution inside opaque plastic boxes (50 cm in length \times 30 cm in width \times 15 cm in height; 20 L).

The nutrient solution was adapted from Banhos et al. (2016) and shows a chemical composition based on the solution proposed by Clark (1975), having been used to test Al resistance in *Citrus* rootstocks (Santos et al. 2000; Banhos et al. 2016). It is consisted of 1372.8 μM $\text{Ca}(\text{NO}_3)_2 \cdot 4\text{H}_2\text{O}$, 507 μM NH_4NO_3 , 224.4 μM KCl, 227.2 μM K_2SO_4 , 218.6 μM KNO_3 , 483.2 μM $\text{Mg}(\text{NO}_3)_2 \cdot 6\text{H}_2\text{O}$, 12.9 μM KH_2PO_4 , 26.01 μM $\text{FeSO}_4 \cdot 7\text{H}_2\text{O}$, 23.8 μM NaEDTA, 3.5 μM $\text{MnCl}_2 \cdot 4\text{H}_2\text{O}$, 9.9 μM H_3BO_3 , 0.9 μM $\text{ZnSO}_4 \cdot 7\text{H}_2\text{O}$, 0.2 μM $\text{CuSO}_4 \cdot 5\text{H}_2\text{O}$, 0.4 μM $\text{NaMoO}_2 \cdot 2\text{H}_2\text{O}$. In a previous

study (Banhos et al. 2016), we observed that 1480 μM Al causes Al-induced decrease in gas exchange rates in ‘Rangpur’ lime plants after 45 days. Therefore, besides macro and micronutrients, this solution contained 0, 370, 740, 1110 and 1480 μM Al provided through $\text{AlCl}_3 \cdot 6 \text{H}_2\text{O}$. The pH of the solution was monitored daily and maintained at 4.0 ± 0.1 to keep Al as soluble as possible, and the solution was totally replaced every 15 days. The nominal chemical composition of this solution was also tested on Geochem-EZ software (Shaff et al. 2010), resulting in more than 85% free Al^{3+} available. We also measured Al in the solutions using the colorimetric method (Sarruge and Haag 1974), and nominal 370, 740, 1110 and 1480 μM Al supply resulted in 214.4 ± 32.6 , 400.2 ± 32.8 , 907.7 ± 42.9 and 981.6 ± 67.9 μM Al.

Expanded polystyrene (Isopor®) 50 × 30 cm plates (2 cm thick), with eight holes (2.5 cm in diameter) each, were floated on the nutrient solution in the boxes, and the plants were fixed in these holes with polyurethane foam strips that were placed around the plant collar. The boxes stayed on benches (80 cm from the ground) inside a greenhouse under semi-controlled conditions (air temperature 28.5 ± 0.7 °C; relative humidity $63.3 \pm 1.3\%$; 853.4 ± 175.1 $\mu\text{mol photons m}^{-2} \text{ s}^{-1}$; approximately 14 h of natural photoperiod).

Experimental design

After separating a group of plants for initial measurements [biometric data (leaf area, number of leaves per plant, shoot length and main root length per plant) and biomass of organs], we set up the plants in the hydroponic system, and measured the accumulated length of the main root every 7 days until 60 days after planting (DAP), when biometric data, as well as the biomass of organs, were assessed again.

Using plants grown in the most contrasting treatments (0 and 1480 μM Al), we collected root tips to measure the concentration of IAA at 1, 3, 7, 15, 30 and 60 DAP. After having conducted a transcriptome analysis using ‘Rangpur’ lime plants grown under 0 and 1480 μM Al, in the present study we collected root tips at 1, 7, 15, 30 and 60 DAP to assess the expression of some genes that had been differentially expressed and revealed by the transcriptome analysis (Table S1; Supplementary material). These were the *Cl-MATE* (multidrug and toxic compound exudation), *Cl-CS* (citrate synthase), *Cl-SAUR 10* and *Cl-SAUR 15* (small auxin up-regulated RNAs) and *Cl-PMEI*. The *Cl-MATE* gene family encodes membrane proteins that facilitate the secretion of organic anions such as citrate that chelates Al in the apoplast (Liu et al. 2009). The SAUR gene family is responsible for acidification of the apoplast during IAA action (Spartz et al. 2014). The *Cl-SAUR 10* showed close identity when compared to *Gm-SAUR X10A*, and *Cl-SAUR 15* had high identity when compared to *Gm-SAUR 15A*, being

Gm-SAUR X10A and *Gm-SAUR 15A* the first characterized SAUR genes, both evidenced in *Glycine max* (McClure et al. 1989), which share similar functions in elongating tissues responding to auxin within few minutes (Jain et al. 2006). PMEI inhibits demethylesterification of pectic carboxylic groups in cell walls of root cells, which occurs through the action of PME (Giovane et al. 2004).

To check whether organic acids (OAs) were being synthesized and secreted by the roots, we cultivated a group of plants showing the same age and height as described above in the same nutrient solutions as previously described (Banhos et al. 2016). The plants were cultivated in 50 mL Falcon® tubes containing the nutrient solutions (45 mL) with 0 and 1480 μM Al for seven days. The tubes were wrapped with aluminum foil to avoid light to the nutrient solution, and were kept in racks, on benches in the lab, under controlled conditions (25 ± 1 °C; 600 $\mu\text{mol photons m}^{-2} \text{ s}^{-1}$; 12 h of photoperiod). The plants were fixed at the mouth of the tubes using polyurethane foam strips that were placed around the plant collar. The pH of the solution in each tube was monitored daily and maintained at 4.0 ± 0.1 to keep Al as soluble as possible. Aeration of the solution in each tube was performed using aquarium pumps. The nutrient solution was not replaced in the tubes, and deionized water was added to each tube to complete the 45 mL every day. After seven days, we quantified oxalic, succinic, malic and citric acids in the nutrient solution and in the root tips using a gas chromatograph coupled to a mass spectrometer (GC–MS).

In addition, we collected root tips at 7, 15, 30 and 60 DAP to conduct anatomical analyses of plants grown under 0 and 1480 μM Al in order to check anatomical disorders during the period of exposure to Al.

Biometric parameters

The lengths (cm) of roots (from the plant collar to the root tip) and stems (from the plant collar to the shoot apex) were measured with a ruler, and the number of leaves was counted. At 0 DAP (for initial measurements) and at the end of the study (60 DAP), plants were separated into leaves, stems (plus petioles) and roots. The leaf area (cm^2) was measured with an area meter (LI-3100C, LI-COR, USA). The organs were dried at 60 °C until constant mass to obtain the biomass (g) of organs and total plant biomass.

Indole-acetic acid analysis

Extraction and purification

Root apices (0.5 cm in length) were washed in deionized water and stored at -80 °C prior to analysis. Samples (420 μg fresh weight) were extracted using isopropanol:acetic acid (95:5; v:v) solution at 4 °C. A

solution containing 0.5 µg of a labelled standard [$^{13}\text{C}_6$]-IAA (Cambridge Isotopes, Inc.) was added as internal standard (IS). After 2 h, the solvent was separated by centrifugation at 14,000×g for 10 min at 4 °C. The supernatant was concentrated to 50 µL, acidified to pH 2.5, and IAA was extracted three times with ethyl acetate, according to Ludwig-Müller et al. (2008). After purification, the solution was evaporated to dryness and re-suspended in 30 µL ethyl acetate for methylation with diazomethane.

GC-MS analysis

Quantification of free IAA was performed using gas chromatography coupled with mass spectrometry: a Hewlett Packard 6890 gas chromatograph (GC) coupled to an HP5973 mass selective detector. The GC column was HP-1701 (30 m, 0.25 mm I.D., 0.5 µm film thickness), with helium as the carrier gas at flow rate of 1 mL min⁻¹. The temperature program for analysis was 140 °C for 1 min, followed by increase of 5 °C min⁻¹ up to 210 °C, 1 min hold, increase to 280 °C at 20 °C min⁻¹ then 1 min hold at 280 °C. The ions were monitored at m/z 130 and 189, for the endogenous IAA, and m/z 136 and 195, for the labeled IS. The ratio 130:136 was used to calculate the endogenous amount of IAA.

RNA extraction and transcriptome analysis

Root apices were collected, frozen in liquid nitrogen (N₂) and RNA was extracted using the RNeasy plant mini kit (Qiagen, Hilden, Germany). Total RNA was precipitated with sodium acetate and ethanol. All samples had a A260/A280 nm ratio > 1.99. Samples were sent to transcriptome sequencing (RNA-seq) at BGI (Beijing, China).

Three samples (bulk of root apices at 0 and 1480 µM Al) were used for library construction, quality assessment (Agilent 2100 Bioanalyzer) and RNA sequencing in an Illumina HiSeq2000 equipment (100 bp, pair-end sequencing). Raw reads from Illumina sequencing were submitted to quality control tests using FASTQC (v. 0.11.5) (Andrews 2010) prior to analysis. GC biased regions were removed using Fastx Trimmer (Fast Tool Kit package v. 0.0.14—McKenna et al. 2010) and filtering by size and quality using Seqclean (v. 1.9.12) (Zhbannikov et al. 2017). Base trimming was done from the 3' and 5' end of each read to remove bases with a quality below Q30. Reads shorter than 30 bp and the remaining orphan reads were removed before further analysis.

Clean reads were mapped in *Citrus sinensis* cDNA library available at “*C. sinensis* Annotation Project” (Wang et al. 2014) using Bowtie2 (v. 2.2.6) (Langmead and Salzberg 2012) according to its default parameters and they were counted using RSEM (Li and Dewey 2011). Differential

expression analysis using TPM (Transcripts per million—Wagner et al. 2012) was performed using NOISeq package (v. 2.14.1) (Tarazona et al. 2011), a non-parametric approach for the identification of differentially expressed genes from count data with the ability to simulate replicates.

The log ratio (M) and the absolute value of difference (D) were estimated to collect the information on fold change and also the absolute pseudo-counts difference. Read counts of each library mapped to the *C. sinensis* cDNA library were used for the differential expression analysis. Lists of counting that were differentially expressed at significant level ($q=0.9$ and $\text{prob}>0.9$) were used for further analysis.

Gene expression analysis

We used quantitative PCR to analyze the expression of *Cl-MATE*, *Cl-CS*, *Cl-SAUR 10*, *Cl-SAUR 15* and *Cl-PMEI*, which had been differentially expressed in the presence of Al as revealed by the transcriptome analysis (Table S1; Supplementary material). Based on RNA-seq data, we designed primers to *Cl-MATE* (forward CATTGACACAGCATTTATCGGC and reverse CAAATGAGGTTGTAATATTAACATAATGGG), *Cl-CS* (forward CGCTAAGCCAGATGGAGAAC and reverse ACAGTGGCAGCATCTCTCAA), *Cl-PMEI* (forward CCACAAGAACGACAGCGATA and reverse TTAGCGTAACTCGGCAAGGT), *Cl-SAUR 10* (forward TGGGTTTCAACTCACAAGC and reverse TGAACAATAACAGGCAAACG) and *Cl-SAUR 15* (forward AGGCGTGCTCTTATGGTTTC and reverse TTCTGAAAGGATGGGTGCTT). As reference genes we used *GAPC2* (forward TCCTATGTTTGTGTTGGGTG and reverse GGTCATCAAACCCTCAACAA) and *EFA* (forward TCAGGCAAGGAGCTTGAGAAG and reverse GGCTTGGTGGGAATCATCTTAA), which were proposed by Mafra et al. (2012) (Mafra et al. 2012).

Serial dilutions of genomic DNA from *C. limonia* were amplified using the internal primers in order to assess the amplification efficiency during qPCR analysis. GoTaq qPCR Master Mix (Promega, Madison, USA) was used as the reagent in these tests, with the following procedural specifications: 95 °C for 5 min (1 cycle), 95 °C for 10 s, 58 °C for 30 s, 72 °C for 30 s (40 cycles) followed by a melting curve analysis (1% slope temperature; 60–95 °C). Amplification efficiencies were 91.85% for *Cl-MATE*, 85.38% for *Cl-CS*, 97.22% for *Cl-PMEI*, 91.71% for *Cl-SAUR 10*, 91.55% for *Cl-SAUR 15*, 97.24% for *Cl-GAPC2* and 100.04% for *Cl-EFA*.

For quantitative analysis of gene expression, total RNA was extracted from root samples using the RNeasy plant mini kit (Qiagen, Hilden, Germany). Total RNA (2 µg) was treated with RNase-free TURBO DNase (Ambion, Carlsbad, USA) and transcribed in reverse to cDNA using an oligo-dT primer and Super Script III, according to the manufacturer's

protocol (Life Technologies, Carlsbad, USA). cDNAs were submitted to gene expression analysis using GAPC2 and the EF α genes in order to normalize the cycle threshold (Ct) values. The reagent and cycles used for the qRT-PCR analyses were the same as those used for the amplification efficiency tests. In this protocol, every reaction was performed in triplicate.

Ct value of each sample, determined by the mean of the three technical replicates, was converted into relative quantities (RQ) using the function $RQ = E^{\Delta Ct}$. ΔCt is the difference between the lowest Ct value across all samples for the evaluated gene and the Ct value of the given sample. A normalization factor (NF) for each sample was calculated by the geometric mean of the RQ values of GAPC2 and EF α . Normalized-relative quantity (NRQ) of each sample was calculated as the ratio of the sample RQ and the appropriate NF. Individual fold change values were determined by dividing the sample NRQ by mean values of NRQ that were obtained from the calibrator, i.e., root samples of plants not exposed to Al. Following this, fold change in the control group always shows a mean value of 1.

Oxalic, succinic, malic and citric acids analyses

Standard curves

To check the method and the GC-MS ability to detect, separate and quantify the OAs, we set up standard curves for each OA by adding six concentrations (5, 10, 30, 50, 70 and 100 $\mu\text{g mL}^{-1}$) of oxalic (Merck, Germany), succinic (Merck, Germany), malic (Fluka – Thermo Fisher Scientific, USA), and monohydrated citric (Fluka—Thermo Fisher Scientific, USA) standard acids in methanol. In order to establish a relationship between GC-MS peak areas and the OAs concentrations found in the nutrient solution with 0 and 1480 μM Al, we set up three standard curves for each OA by adding six concentrations (25, 50, 100, 200, 300 and 400 $\mu\text{g mL}^{-1}$) of the oxalic, succinic, malic and citric standard acids. For each concentration, three replicates were used and values were plotted to generate the standard curves, and the equations with their respective R^2 are shown in Table S2 (Supplementary material).

Secreted organic acids and their contents in roots tips

For measuring the secreted OAs, the solutions (45 mL) in the Falcon tubes were dried in a forced-air oven at 80 °C and the OAs, concentrated. Volatizing temperatures of none of the OAs are above 80 °C. For measuring OAs contents in the root tips, they were extracted by osmosis and alkaline gradient, immersing the root tips (0.5 ± 0.1 cm in length) in 1.5 mL 40 mM Na_2CO_3 for 24 h. Then, 1 mL of the

extracting solution was collected and dried completely at 80 °C. Samples were esterified according to Fischer method (methylation) (Fischer and Speier 1895). We added 700 μL of methanol (HPLC/Spectro) and 300 μL of sulphuric acid (7 N) in the secreted OAs samples, and 400 μL of methanol (HPLC/Spectro) and 100 μL of sulphuric acid (7 N) in the concentrated samples resulting from the extraction of OAs from root tips. Both sample types were shaken and kept for 1 h at 70 °C for catalysing the reaction. After adding 1 mL of hexane (HPLC/Spectro), 100 μL of the apolar phase were collected and analyzed using a GC-MS system (GC-2010/GCMSQP2010 Plus, Shimadzu, Japan), with an automatic sample injector (AOC-20i).

GC-MS parameters

In the GC-MS, we used a 30 m-length and 250 μm -diameter fused-silica microcolumn (RTX-5MS, Restek), and analytical ultra-pure helium (99.9999%, White Martins) was used as carrier gas. The injector temperature was 250 °C (Splitless mode) and the injection volume was 1 μL . Column gas flow was maintained at 41 cm s^{-1} . The initial column temperature was 50 °C with a 4 min step. After that, at a 10 °C min^{-1} rate, it achieved 70 °C. Then, it was increased to 250 °C at a 25 °C min^{-1} rate, and maintained for 0.8 min, completing 14 min running. Mass detector was a simple quadrupole type with 70 eV electronic impact ionization. The GC-MS interface temperature was 250 °C and 230 °C to the ionizer. The detector potential was relative to tuning, with a 40 to 450 m/z detection range (scanner mode).

Anatomical analysis

Root tips (~0.5 cm in length and 1 mm in diameter) were collected and immediately fixed in Karnovsky solution (Karnovsky 1965). The samples were dehydrated in increasing ethanol series [30, 50, 70, 90 (one hour each), and 100% (three times, one hour each)], then infiltrated with resin (Historesin, Leica instruments, Germany) and ethanol 100%, at a ratio of 1:1, overnight. After 24 h, samples were infiltrated with pure resin, reserved overnight and then polymerized in blocks. Longitudinal sections were obtained with a rotary microtome and mounted on permanent glass slides that were immersed (5 min) in a toluidine blue solution (pH 4.5) for staining (at room temperature) structures containing nucleic acids and lignin (O'Brien et al. 1964). Then, the glass slides were washed under tap water to remove excess of dye and dried with a clean cotton cloth.

All sections were observed under light microscope (DMLB, Leica Microsystems, Wetzlar, Germany) and the images were captured with a digital camera (DFC-290, Leica Microsystems, Germany) functionally attached to the DMLB.

The anatomical study was based on consecutively-sliced longitudinal sections of root tips containing the root cap, the quiescent center, and elongation, division and maturation zones.

Data analysis

Biometric data and the biomass of organs were measured using eight replicates (plants). Concentration of IAA in the root tips was evaluated using three plants. For gene expression and OAs quantification in root tips and in the solution, five samples were used as replicates.

A one-way analysis of variance (Anova) was performed between plants exposed to 0, 370, 740, 1110 and 1480 μM Al to test for differences in accumulated main root length at every evaluation date. The Tukey test ($\alpha=0.05$) was used to conduct post-hoc comparisons to estimate the least significant differences between mean results. Biometric data and biomass of organs were subjected to student's *t* test ($\alpha=0.05$) to verify differences between 0 and 60 DAP within each Al concentration. This same test was used to verify differences in IAA concentration, expression of genes and OAs synthesis/release between 0 and 1480 μM Al on distinct evaluation dates.

Results

Effects of Al on plant growth

Plants showed reduced plant growth, fewer leaves and decreased root development with the increase of Al concentration in the nutrient solution (Fig. 1). Differences in root growth started after 14 DAP. At 21 and 28 DAP, plants exposed to Al showed similar values that were lower than those of plants not exposed to Al. From 35 DAP until 56 DAP, plants exposed to 370 μM Al emerged as an intermediate treatment, showing values that were lower than those of plants not exposed to Al but higher than those of plants exposed to 740, 1110 and 1480 μM Al (Fig. 2).

When compared to initial values (0 DAP), the increment of leaf area (Fig. 3a), number of leaves (Fig. 3b), shoot length (Fig. 3c) and main root length (Fig. 3d) within 60 days reduced considerably with the increase of Al concentration in the nutrient solution. Plant biomass exhibited the same response pattern, showing reduced values of leaf (Fig. 4a), stem (plus petioles) (Fig. 4b), root (Fig. 4c), and total biomass (Fig. 4d) with the increase of Al concentration in the nutrient solution.



Fig. 1 General view of the root system of 'Rangpur' lime plants grown for 60 days in nutrient solutions containing 0, 370, 740, 1110 and 1480 μM Al

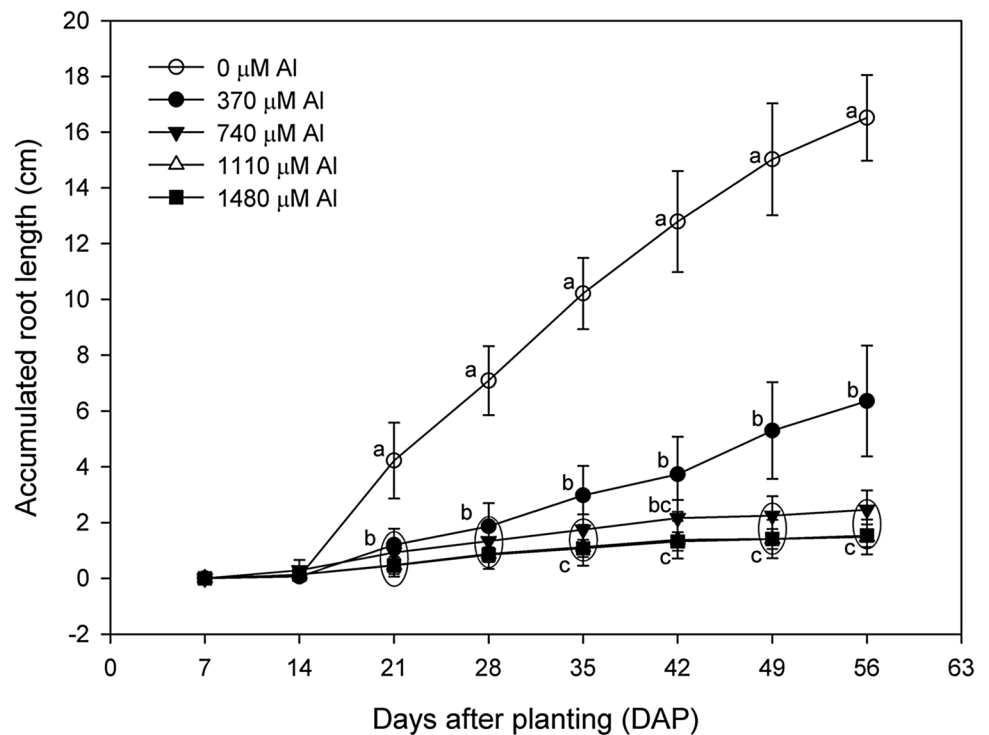
Effects of Al on root IAA content

Plants exposed to 1480 μM Al showed higher IAA concentration in their root tips when compared to plants not exposed to Al, mainly at 3, 7 and 15 DAP (Fig. 5). After 15 days, IAA concentration in root tips of plants exposed to Al became similar to those of plants not exposed to Al (Fig. 5).

Effects of Al on gene expression

The transcriptome analysis of plants grown in the presence and absence of Al did not show differential expression of genes responsible for membrane proteins associated with auxin polar transport, such as AUX1, AUX2 and PINs (Table S1; Supplementary material). When exposed to 1480 μM Al, the gene responsible for *Cl-MATE* channel was 10.4 and 1.5 times more expressed at 1 and 7 DAP, respectively (Fig. 6a). However, at 60 DAP, *Cl-MATE* was 215 times more expressed in plants exposed to Al when compared to plants not exposed to Al (Fig. 6a). *C. limonia* citrate synthase gene expression was down-regulated at 15 DAP (1.6 times less expressed) and 30 DAP (5.3 times less expressed) in the presence of Al in relation to plants not exposed to Al. However, *Cl-CS* was considerably up-regulated (9.1 times more transcripts) in the presence of Al at 60 DAP (Fig. 6b). *Cl-PMEI* gene expression, however, showed up-regulation at 7 DAP (1.8 times more transcripts), and then became down-regulated in response to Al, reducing to 3.4 (15 DAP), 10 (30 DAP) and 20 times less transcripts (60 DAP) in relation to plants not exposed to Al (Fig. 6c). The same up-regulation followed by down-regulation response pattern was observed for *Cl-SAUR 10*, which was 2.8 times

Fig. 2 Accumulated length of the main root of ‘Rangpur’ lime plants grown for 56 days in nutrient solutions containing 0, 370, 740, 1110 and 1480 μM Al. For each evaluation date, different letters represent significant differences ($P < 0.05$) between Al concentrations. Bars = S.D



more expressed at 7 DAP and reduced to 25 times less transcripts at 60 DAP (Fig. 7a). *Cl-SAU15* followed a similar response, showing down-regulation at 15 DAP (2 times less transcripts) and 60 DAP (33.3 times less transcripts) (Fig. 7b).

Effects of Al on organic acids in the root tips and secreted in the solution

OAs contents were found in root tips of all plants after 7 days. However, in relation to plants not exposed to Al, only succinate was significantly reduced in root tips of plants exposed to Al (Fig. 8a). After 7 days, oxalate, succinate and citrate were detected in the nutrient solutions and were higher in the solutions containing Al. Citrate was not found in the solution absent in Al, but in the solution containing Al approximately $9 \mu\text{mol citrate g}^{-1} \text{FW}$ was secreted (Fig. 8b).

Effects of Al on anatomical characteristics of root tips

In plants not exposed to Al, cells with regular size and rectangular shape were noted in the cortex (Fig. 9b), while in plants exposed to 1480 μM Al, thick non-uniform round shape cells were found in the cortex (Fig. 9d), after 15 days of Al exposure. This anatomical pattern was reflected in the shape of the extreme root tip as plants exposed to Al showed a wider root tip (Fig. 9c, g, k) when compared to a sharp arrow-like root tip in plants not exposed to Al (Fig. 9a, e, i).

When exposed to Al, more lignin deposition was observed in the vascular cylinder, as evidenced by stronger blue-green stains (Fig. 9d). The longer the exposure time to Al, the more apparent became this lignin deposition in the vascular cylinder (Fig. 9d, h, l). Anatomical ruptures could be observed on root epidermis of plants exposed to Al, mainly after 30 and 60 days of Al exposure (Fig. 9g, k), indicating an irregular pattern of epidermal cell division and elongation, which contrasted with plants not exposed to Al (Fig. 9e, f).

Discussion

‘Rangpur’ lime plants are sensitive to Al (Santos et al. 2000; Pereira et al. 2003; Banhos et al. 2016) and here we show that, although they possess genes associated with Al resistance, as revealed by the transcriptome analysis (Table S1; Supplementary material), their expression is not consistent over time of Al exposure. *Cl-MATE* and *Cl-CS* were conspicuously up-regulated when the roots were exposed to 1480 μM Al, but only at 60 DAP. In addition, we confirmed that ‘Rangpur’ lime plants had OAs inside their roots independently of the Al presence (Fig. 8a). These OAs are broadly known to be synthesized in the Krebs’ cycle, which takes place in the mitochondria. In fact, the presence of mitochondria in root tips of *Citrus grandis* and *C. sinensis* has been evidenced (Huang et al. 2014). After seven days, except for malate, OAs were significantly higher in

Fig. 3 Leaf area, number of leaves, shoot and root length of ‘Rangpur’ lime plants at 0 and 60 days after planting (DAP), grown in nutrient solutions containing 0, 370, 740, 1110 and 1480 μM Al. For each Al concentration, asterisks represent significant differences ($P < 0.05$) between 0 and 60 DAP. Bars = S.D

the solution containing Al, indicating that OAs, including citrate, are secreted by this species in response to Al. Citrate secretion is mediated by *MATE* (Furukawa et al. 2007), and a cluster analysis of the *MATE* sequence found showed highest phylogenetic proximity to *MATE* genes related with this same function in different species (data not shown). CS and *MATE* can be both up-regulated by Al (Xu et al. 2010), but in transformant tobacco plants CS expression did not lead to the efflux of citrate by *MATE* channels (Delhaize et al. 2001), while in barley only citrate secretion responds to Al (Zhao et al. 2003), indicating there is no consistent pattern in the expression of *MATE* and CS in response to Al. In the present study, *Cl-CS* and *Cl-MATE* were concomitantly up-regulated at 60 DAP, indicating a consistent pattern in the expression of these two genes in response to Al. Therefore, for ‘Rangpur’ lime plants, Al seems to induce CS and *MATE* gene expression, leading to an increase in OA contents in roots, although the timing of these events seems to be ineffective against Al.

In soybean plants, a 16% increase in citrate synthase activity occurred upon Al treatments after 6 h (Xu et al. 2010). In *Vigna umbellata*, the citrate secretion mediated by *MATE* also occurred 6 h following Al exposure (Liu et al. 2013). In the present study, *Cl-CS* was not significantly up-regulated at 7 DAP (Fig. 6b) corroborating the similar citrate concentration in root tips of both treatments (Fig. 8a). However, approximately 9 μmol citrate per g FW was secreted in the solution containing Al, at 7 DAP (Fig. 8b). Excised roots of *Citrus grandis* and *C. sinensis* exposed to 500 μM Al reached a peak of 0.7 μmol citrate per g FW after 24 h (Yang et al. 2011), while in the present study the citrate secretion was ten times higher. This can be explained by the fact that we used whole plants with their intact root system exposed to a three times higher Al concentration during a period of Al exposure that was seven times longer. In addition, after reaching a peak of citrate secretion, excised roots decrease the secretion of OAs, as evidenced in *Citrus grandis* and *C. sinensis* (Yang et al. 2011), perhaps because excised roots cannot maintain the same metabolism as entire plants. In the case of the whole root system of ‘Rangpur’ lime plants, the up-regulation of *Cl-MATE* and *Cl-CS* only at 60 DAP may be a delayed response to mitigate the effects of Al, and investigation of OAs concentration in root tips and released in the solution over time of Al exposure merits further investigation. Therefore, in the present study, it seems that gene expression of *Cl-MATE* and *Cl-CS* was too low and too late, and OAs released in the solution could be too

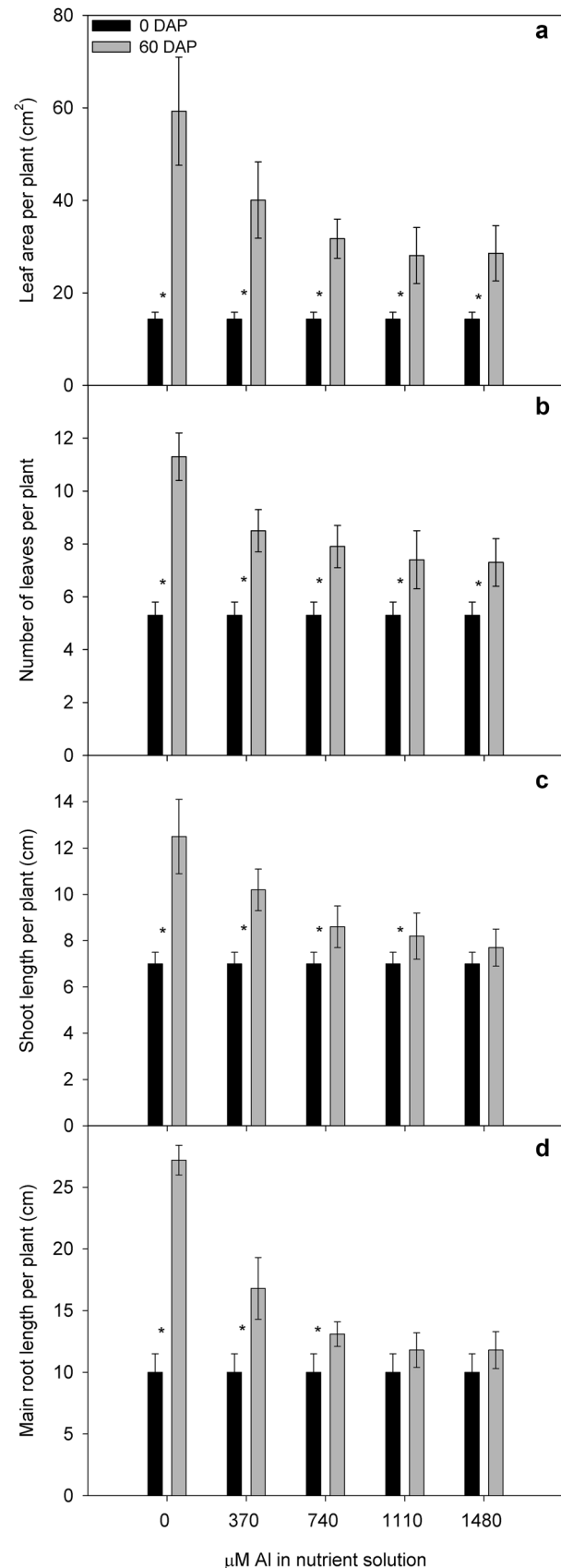


Fig. 4 Biomass of leaves, stems (plus petioles), roots, and total biomass of ‘Rangpur’ lime plants at 0 and 60 days after planting (DAP), grown in nutrient solutions containing 0, 370, 740, 1110 and 1480 μM Al. For each Al concentration, asterisks represent significant differences ($P < 0.05$) between 0 and 60 DAP. Bars = S.D

low to counter Al effects, so that Al caused tissue damage already observed from 15 DAP (Fig. 9). Still, OAs secreted by the plants could be diluted in the nutrient solution, while in the soil, the rhizosphere could have a different benefit of OAs secretion. Notwithstanding, as far as we are aware, this possibility has never been checked and most studies of OA secretion are performed for a short period of time (maximum 48 h), many of them with excised roots, without association with other physiological responses. Then, further investigation is necessary in this matter.

On the other hand, *Cl-PMEI*, the inhibitor of demethylesterification, was up-regulated at 7 DAP, but became down-regulated at 15, 30 and 60 DAP (Fig. 6c). Thus, at least until 7 DAP pectic carboxylic groups in the cell wall were protected from demethylesterification that could expose free pectic carboxylic groups, which could serve as binding sites for Al in the wall (Zhu et al. 2014). For instance, potato transformants that exhibited higher expression of PME accumulate more Al, produce more callose and their root growth is more inhibited when exposed to Al than wild types (Schmohl et al. 2000). After 15 days, when *Cl-PMEI* was down-regulated, the binding sites for Al in the wall became unprotected, and demethylesterification was likely to act in these conditions. Demethylesterification occurs within hours (Franco et al. 2002). Therefore, the up-regulation of a gene encoding inhibitors of demethylesterification only at 7 DAP may not be considered a fast response, even in a 60-day experiment. Then, the down-regulation of *Cl-PMEI* (after 15 days), could have allowed increased demethylesterification and Al binding to the cell wall, and this fact could explain why roots of plants exposed to Al showed 10 times higher Al concentration when compared to those of plants not exposed to Al, after 60 days (Fig. S1, Supplementary Material). This same pattern of Al accumulation in roots of plants exposed to Al has already been evidenced for other *Citrus* plants (Yang et al. 2011), including *C. limonia* (Banhos et al. 2016). Taken together, *Cl-PMEI* up-regulation at 7 DAP (but down-regulation from 15 to 60 DAP), while *Cl-MATE* and *Cl-CS* increased expression only at 60 DAP could indicate that the response of these genes is not only delayed (*Cl-CS* and *Cl-MATE*) but their timing seems to be ineffective against Al, and this may explain the Al sensitivity in this species.

We confirmed that Al interferes with root elongation and root biomass production in ‘Rangpur’ lime plants. Plants not exposed to Al showed accumulated root length that was 10 times higher than that of plants exposed to 370 μM Al, and

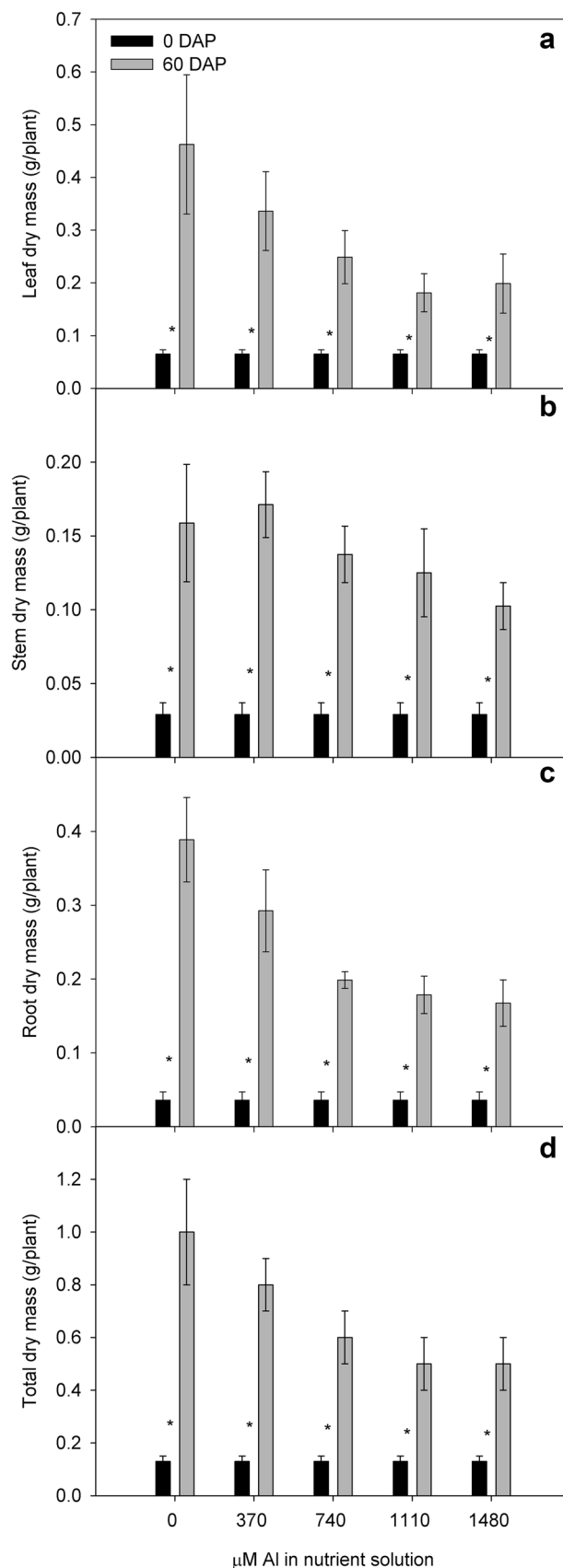
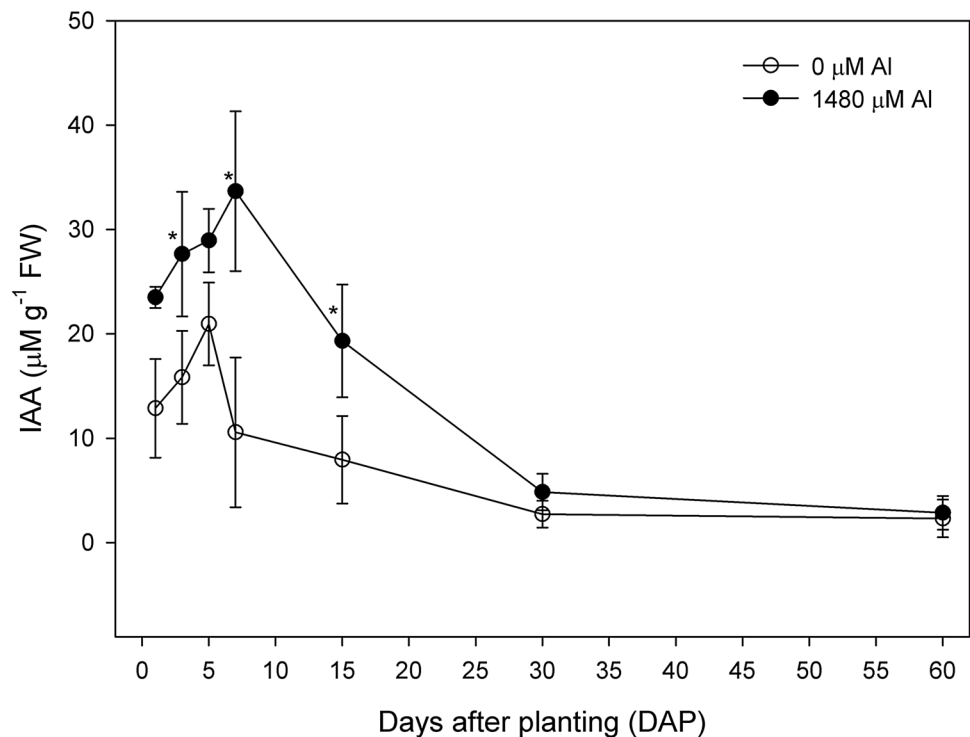


Fig. 5 Indol-acetic acid (IAA) concentration measured in root tips of ‘Rangpur’ lime plants grown in nutrient solutions containing 0 and 1480 μM Al at 1, 3, 7, 15, 30 and 60 days after planting (DAP). For each evaluation date, asterisks represent significant difference ($P < 0.05$) between 0 and 1480 μM Al. Bars = S.D



16 times higher when compared to plants exposed to 740, 1110 and 1480 μM Al, at 56 DAP (Fig. 2). These expected symptoms, however, were accompanied by high concentration of IAA in root tips of plants exposed to Al, mainly at 3, 7 and 15 DAP (Fig. 5). In *Arabidopsis*, Al was also found to induce a localized enhancement of auxin biosynthesis in the root apex, leading to inhibition of root growth (Yang et al. 2014). Differently from stems, in cells (of the elongation zone) of root tips, high concentration of IAA can cause strong inhibition of cell elongation (Rahman et al. 2007; Cleland 2010). IAA concentration in root tips of plants exposed to Al was three- (7 DAP) and two-fold higher (15 DAP) than that of plants not exposed to Al (Fig. 5). Intriguingly, the expression of *Cl-SAUR 10* was also up-regulated at 7 DAP, when a peak of IAA concentration occurred in plants exposed to Al (Fig. 5) after which this gene became down-regulated until the end of the study, similar to what occurred with *Cl-SAUR 15* gene expression and IAA contents, which became similar to the root tips of plants not exposed to Al after 15 days (Fig. 5). This suggests that at least until 7 DAP auxin action occurred as SAUR genes are responsible for acidification of apoplast (Spartz et al. 2014). Alkalinization of the apoplast, on the other hand, is associated with inhibition of root cell elongation under elevated auxin concentration (Lüthen and Böttger 1993; Evans et al. 1994; Hager 2003). Thus, the up-regulation of *Cl-SAUR 10* occurring together with the peak of IAA concentration in roots of plants exposed to Al demonstrates that initially (until 7 DAP), *Cl-SAUR 10* gene expression

was acting towards root cell elongation. However, after the peak of IAA, *Cl-SAUR 10* and *Cl-SAUR 15* gene expressions were down-regulated, suggesting that normal IAA cell elongation stimulus (acidification of apoplast) was not acting anymore while IAA concentration was kept high until 15 DAP (Fig. 5), which might have inhibited cell elongation in a cumulative manner. Moreover, even though root IAA contents became similar between both treatments, after 15 DAP *Cl-SAUR* genes could not act towards apoplast acidification because they were both down-regulated. Accordingly, Al binds covalently to the free pectin nets of the cell wall, making it more rigid and reducing cell elongation (Kopittke et al. 2008; Horst et al. 2010; Blamey et al. 2011). Once Al is firmly bound to the cell apoplast, it is unlikely to be released, even by the citrate secreted from the cells (Rangel et al. 2009). Therefore, even though IAA concentration in the root tips of plants exposed to Al became similar to those of plants not exposed to Al after 15 days, the thick non-uniform and round shape cells found in the cortex of roots exposed to Al are the result of impairments in cell elongation already observed at 15 DAP (Fig. 9d). This indicates that these cells divided in a periclinal manner, contrasting with the rectangular cells in the cortex of roots not exposed to Al (Fig. 9b) that evidences an anticlinal cell division benefiting the normal growth in length.

Hence, the responses of *Cl-SAUR 10* (up-regulation peaked at 7 DAP) and *Cl-SAUR 15* contrast with those of *Cl-CS* and *Cl-MATE* that peaked only at 60 DAP, reinforcing that the timing of these gene responses is ineffective against

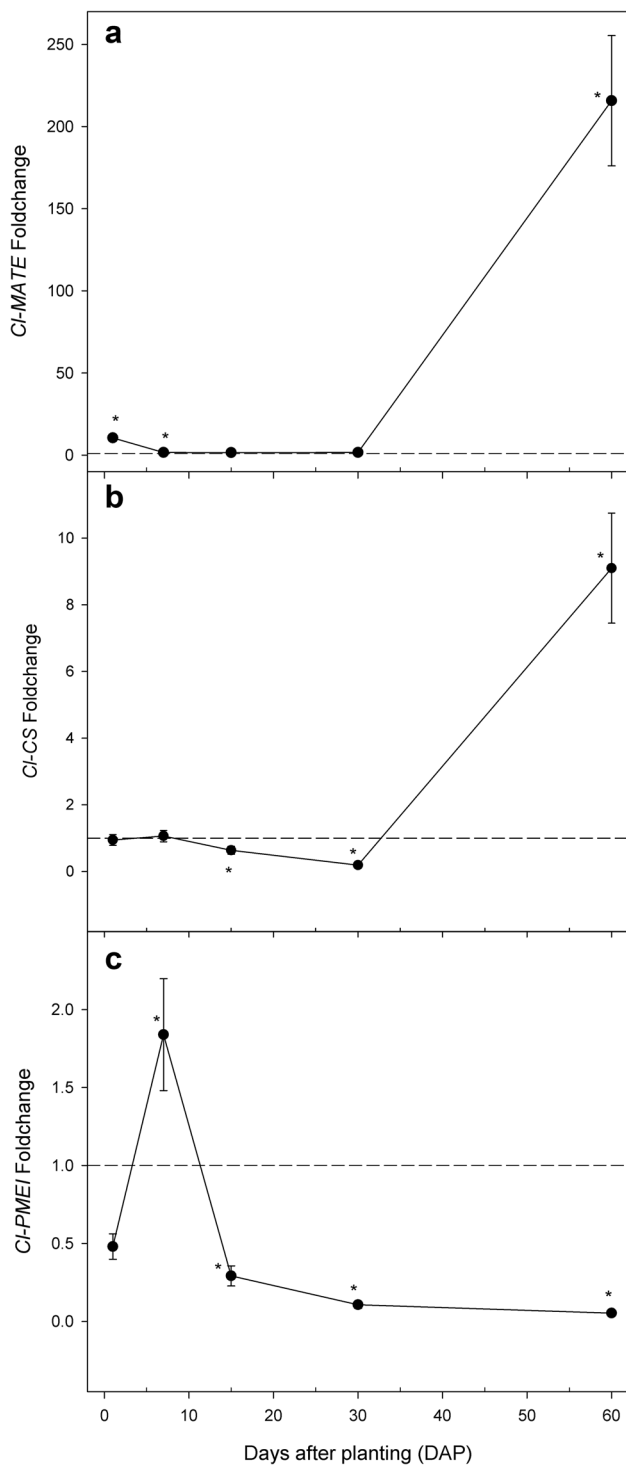


Fig. 6 Gene expression of MATE (multidrug and toxic compound exudation) channel, citrate synthase and pectin methyl esterase inhibitor in root tips of ‘Rangpur’ lime plants grown in nutrient solutions containing 0 and 1480 μM Al at 1, 3, 7, 15, 30 and 60 days after planting (DAP). For each evaluation date, asterisks represent significant difference ($P < 0.05$) between 0 and 1480 μM Al. Dashed line is a reference (one fold change in gene expression of plants not exposed to Al). Bars = S.D

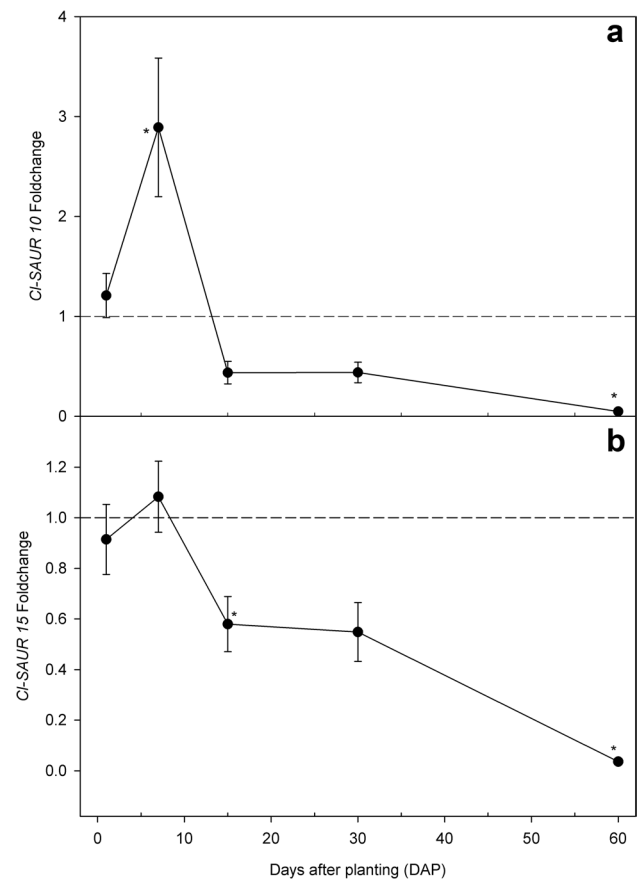


Fig. 7 Gene expression of SAUR (small auxin up-regulated RNAs) in root tips of ‘Rangpur’ lime plants grown in nutrient solutions containing 0 and 1480 μM Al at 1, 3, 7, 15, 30 and 60 days after planting (DAP). For each evaluation date, asterisks indicate significant difference ($P < 0.05$) between 0 and 1480 μM Al. Dashed line is a reference (one fold change in gene expression of plants not exposed to Al). Bars = S.D

Al in ‘Rangpur’ lime plants. In addition, the transcriptome analysis of plants grown in the presence and absence of Al did not reveal any differential expression of genes responsible for membrane proteins associated with auxin polar transport, such as AUX1, AUX2 and PINs (Table S1; Supplementary material). Therefore, in the root tips of ‘Rangpur’ lime plants grown under 1480 μM Al, an increase in IAA concentration, and not an imbalance in IAA distribution, is likely to trigger the inhibition of root cell elongation and, consequently, to reduce the root growth. This is evidenced by round shaped cells in the cortex of roots exposed to Al (Fig. 9d).

Using *Arabidopsis*, Sun et al. (2010) argues that Al-induced ethylene biosynthesis is likely to act as a signal to change auxin distribution in roots by disrupting *At-AUX1* and *At-PIN2*-mediated auxin transport. Such disruption in auxin distribution could lead to asymmetrical auxin distribution and, consequently, twisted root shape, as evidenced by

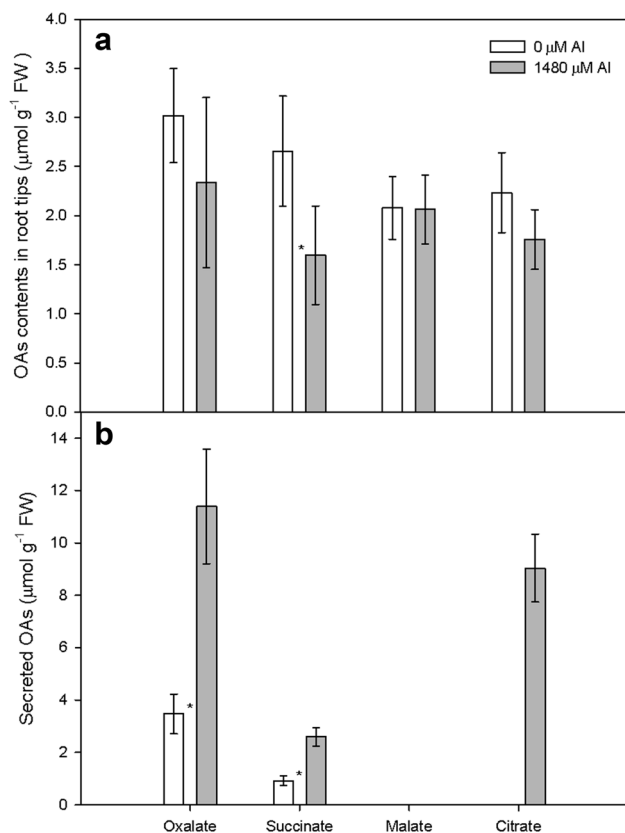


Fig. 8 Organic acids contents in roots tips (a) and released in the nutrient solution (b) by the roots of ‘Rangpur’ lime plants grown for seven days in nutrient solutions containing 0 and 1480 μM Al. For each OA, asterisks indicate significant difference ($P < 0.05$) between 0 and 1480 μM Al. Bars = S.D

Sun et al. (2010). Our anatomical analysis, however, indicated thick non-uniform round shape cells at both sides of the cortex of roots exposed to Al, resulting in a thick growth pattern at the extreme root tip of plants exposed to Al, where no twisted roots were observed on any evaluation date. This observation along with the fact that we did not found differential expression of *AUX1*, *AUX2* and *PINs*, responsible

for auxin polar transport (Table S1; Supplementary material) reinforce that Al-induced high IAA concentration rather than a disruption in IAA distribution occurs in ‘Rangpur’ lime plants exposed to Al.

The ruptures in the epidermis of roots exposed to 1480 μM Al have also been observed in cowpea exposed to 600 μM Al for 48 h (Kopittke et al. 2008; Blamey et al. 2011). These authors argue that these ruptures result from an increase in cell wall rigidity in the outer layers (epidermis and outer portions of the cortex) due to higher Al accumulation in these layers, as observed in barley (Ma et al. 2004) and maize (Stass et al. 2006). According to this, Al reduces elongation in outer layers while cells of the inner root layers continue to elongate, which possibly causes ruptures. We found irregular pattern of epidermal cell division and elongation in roots of plants exposed to Al, contrasting with those of plants not exposed to Al, which could corroborate the explanation given by Kopittke et al. (2008) and Blamey et al. (2011). However, we could not anatomically evidence that the inner root layers are suggestive of regular (anticlinal) cell division, as evidenced by non-rectangular round shaped cells in the whole cortex. Therefore, identifying distinct concentrations of Al in different portions of the root tip of ‘Rangpur’ lime plants exposed to Al is needed in future studies. For example, using Al-specific X-ray coupled to scanning electron microscope (SEM/EDS) enables us to detect the presence of Al in different tissues, as evidenced in leaves of Al-accumulating and non-accumulating species (Bressan et al. 2016).

In this study, we demonstrate that although possessing genes associated with Al resistance, ‘Rangpur’ lime plants are, actually, sensitive to Al and this could be associated with late expression of *Cl-MATE*, *Cl-CS* and *Cl-PMEI* when the roots are exposed to Al in a 60-day study. In addition, we revealed that an increase in IAA concentration in root tips, whether it is due to increased biosynthesis from the root tips or increased transport from above-ground tissues, and not an imbalance in IAA distribution is associated with the inhibition of root cell elongation in this species.

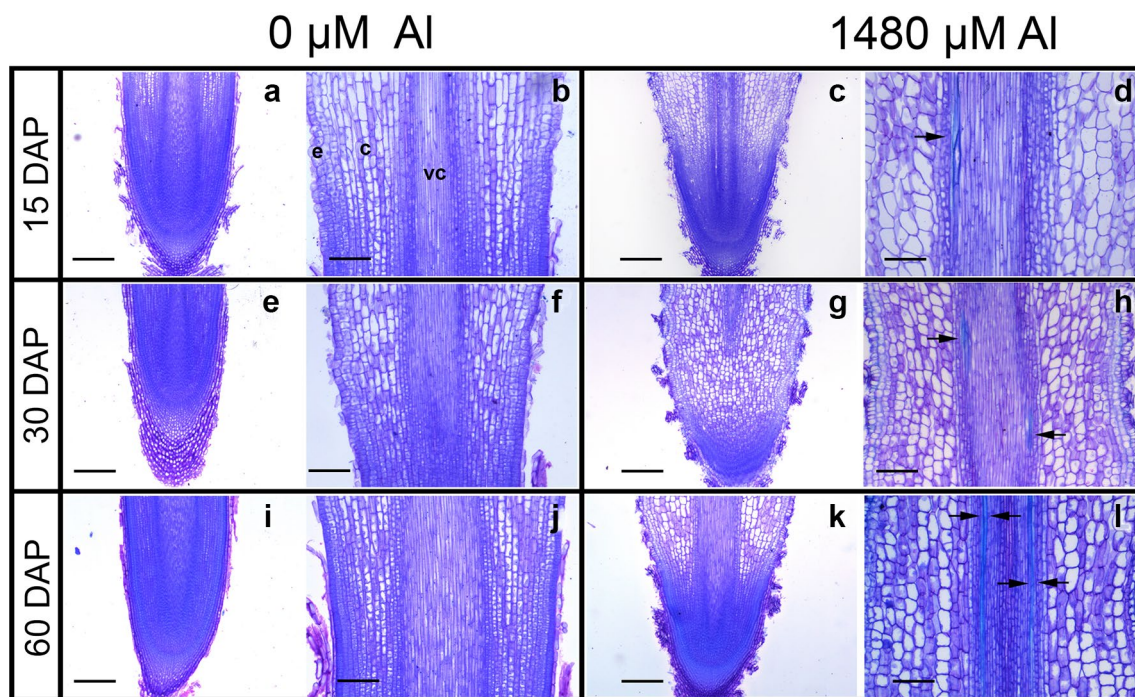


Fig. 9 Anatomical analyses of root tips of ‘Rangpur’ lime plants. **a, b, e, f, i** and **j** grown in nutrient solution containing 0 μM Al; **c, d, g, h, k** and **l** grown in nutrient solution containing 1480 μM Al; **a, e, i, c, g** and **k** root apices; **b, f, j, d, h** and **l** root elongation zone. 15 DAP (**a–d**); 30 DAP (**e–h**); 60 DAP (**i–l**). *c* cortex, *e* epidermis,

vc vascular cylinder. Single arrows: lignin deposition in the vascular cylinder. Double-opposite whole arrows: prominent lignin deposition in the vascular cylinder. Scale bars (μm): **a, c, e, g, i** and **k**=100; **b, d, f, h, j** and **l**=50

Acknowledgements We acknowledge the Brazilian National Council for Scientific and Technological Development (CNPq) for financial support (474169/2013-8 grant to GH), for an undergraduate scholarship to M.F. Cavaleiro and for research fellowships granted to G. Habermann (Grant 309149/2017-7) and E. Purgatto (Grant 305458/2013-2). We extend acknowledgments to the São Paulo Research Foundation (Fapesp) for PhD scholarships granted to C.M.S. da Silva (Fapesp #2013/11370-3), A.C.G. Bressan (Fapesp #2014/14386-0), a MSc scholarship to B.M.O. Carvalho (Fapesp #2016/14216-3) and a grant to E. Purgatto (Fapesp #2013/07914-8), and also to the Coordination for Improvement of Graduate Personnel (Capes) for a PhD scholarship granted to O.F.A.A. Banhos. We thank the Sanicitrus Nursery (Araras, São Paulo state, Brazil) for providing us with the ‘Rangpur’ lime plants.

References

- Andrews S (2010) FastQC: a quality control tool for high throughput sequence data
- Banhos OFAA, Brenda M, de O, da Veiga EB, Bressan ACG, Tanaka FAO, Habermann G (2016) Aluminum-induced decrease in CO₂ assimilation in ‘Rangpur’ lime is associated with low stomatal conductance rather than low photochemical performances. *Sci Hortic* 205:133–140
- Blamey FPC, Kopittke PM, Wehr JB, Menzies NW (2011) Recovery of cowpea seedling roots from exposure to toxic concentrations of trace metals. *Plant soil* 341:423–436
- Bressan ACG, Coan AI, Habermann G (2016) X-ray spectra in SEM and staining with chrome azurol S show Al deposits in leaf tissues of Al-accumulating and non-accumulating plants from the cerrado. *Plant Soil* 404:293–306. <https://doi.org/10.1007/s11104-016-2841-1>
- Brunner I, Sperisen C (2013) Aluminum exclusion and aluminum tolerance in woody plants. *Front Plant Sci* 4:1–12. <https://doi.org/10.3389/fpls.2013.00172>
- Chen L, Qi Y, Liu X-H (2005) Effects of aluminum on light energy utilization and photoprotective systems in citrus leaves. *Ann Bot* 96:35–41
- Clark RB (1975) Characterization of phosphatase of intact maize roots. *J Agric Food Chem* 23:458–460
- Cleland RE (2010) Auxin and cell elongation. In: Davies PJ (ed) *Plant hormones—biosynthesis, signal transduction action!* Springer, Ithaca, pp 204–220
- Delhaize E, Hebb DM, Ryan PR (2001) Expression of a *Pseudomonas aeruginosa* citrate synthase gene in tobacco is not associated with either enhanced citrate accumulation or efflux 1. *Plant Physiol* 125:2059–2067
- Evans ML, Ishikawa H, Estelle MA (1994) Responses of Arabidopsis roots to auxin studied with high temporal resolution: comparison of wild type and auxin-response mutants. *Planta* 194:215–222
- Fischer E, Speier A (1895) Darstellung der ester. *Eur J Inorg Chem* 28:3252–3258
- Franco CR, Chagas AP, Jorge RA (2002) Ion-exchange equilibria with aluminum pectinates. *Colloids Surf A* 204:183–192
- Furukawa J, Yamaji N, Wang H, Mitani N, Murata Y, Sato K, Katsuhara M, Takeda K, Ma JF (2007) An aluminum-activated citrate transporter in barley. *Plant Cell Physiol* 48:1081–1091. <https://doi.org/10.1093/pcp/pcm091>

- Giovane A, Servillo L, Balestrieri C, Raiola A, Avino RD, Tamburrini M (2004) Pectin methylesterase inhibitor. *Biochim Biophys Acta* 1696:245–252. <https://doi.org/10.1016/j.bbapap.2003.08.011>
- Hager A (2003) Role of the plasma membrane H⁺-ATPase in auxin-induced elongation growth: historical and new aspects. *J Plant Research* 116:483–505
- Horst WJ, Wang Y, Eticha D (2010) The role of the root apoplast in aluminium-induced inhibition of root elongation and in aluminium resistance of plants: a review. *Ann Bot* 106:185–197
- Huang J-H, Cai Z-J, Wen S-X, Guo P, Ye X, Lin G-Z, Chen L-S (2014) Effects of boron toxicity on root and leaf anatomy in two *Citrus* species differing in boron tolerance. *Trees* 28:1653–1666
- Jain M, Tyagi AK, Khurana JP (2006) Genome-wide analysis, evolutionary expansion, and expression of early auxin-responsive SAUR gene family in rice (*Oryza sativa*). *Genomics* 88:360–371
- Jiang H-X, Chen L-S, Zheng J-G, Han S, Tang N, Smith BR (2008) Aluminum-induced effects on photosystem II photochemistry in *Citrus* leaves assessed by the chlorophyll a fluorescence transient. *Tree Physiol* 28:1863–1871
- Karnovsky MJ (1965) A formaldehyde-glutaraldehyde fixative of high osmolarity for use in electron microscopy. *J Cell Biol* 27:137–139
- Kochian LV (1995) Cellular mechanisms of aluminum toxicity and resistance in plants. *Ann Rev Plant Biol* 46:237–260
- Kopittke PM, Blamey FPC, Menzies NW (2008) Toxicities of soluble Al, Cu, and La include ruptures to rhizodermal and root cortical cells of cowpea. *Plant Soil* 303:217–227
- Langmead B, Salzberg SL (2012) Fast gapped-read alignment with Bowtie 2. *Nat Methods* 9:357–359
- Li B, Dewey CN (2011) RSEM: Accurate transcript quantification from RNA-Seq data with or without a reference genome. *BMC Bioinform* 12:323–338
- Liu J, Magalhaes JV, Shaff J, Kochian LV, Maize E, Lagoas S, Grosso M (2009) Aluminum-activated citrate and malate transporters from the MATE and ALMT families function independently to confer *Arabidopsis* aluminum tolerance. *Plant J* 57:389–399. <https://doi.org/10.1111/j.1365-3113X.2008.03696.x>
- Liu MY, Chen WW, Xu JM, Fan W, Yang JL, Zheng SJ (2013) The role of VuMATE1 expression in aluminium-inducible citrate secretion in rice bean (*Vigna umbellata*) roots. *J Exp Bot* 64:1795–1804. <https://doi.org/10.1093/jxb/ert039>
- Ludwig-Müller J, Georgiev M, Bley T (2008) Metabolite and hormonal status of hairy root cultures of Devil's claw (*Harpagophytum procumbens*) in flasks and in a bubble column bioreactor. *Process Biochem* 43:15–23
- Lüthen H, Böttger M (1993) The role of protons in the auxin-induced root growth inhibition—A critical reexamination. *Plant Biology* 106:58–63
- Ma JF (2000) Role of organic acids in detoxification of aluminum in higher plants. *Plant Cell Physiol* 41:383–390
- Ma JF, Nagao S, Sato K, Ito H, Furukawa J, Takeda K (2004) Molecular mapping of a gene responsible for Al-activated secretion of citrate in barley. *J Exp Bot* 55:1335–1341. <https://doi.org/10.1093/jxb/erh152>
- Mafra V, Kubo KS, Alves-Ferreira M, Ribeiro-Alves M, Stuart RM, Boava LP, Rodrigues CM, Machado MA (2012) Reference genes for accurate transcript normalization in citrus genotypes under different experimental conditions. *PLoS ONE* 7:e31263
- Magalhaes JV (2010) How a microbial drug transporter became essential for crop cultivation on acid soils: aluminium tolerance conferred by the multidrug and toxic compound extrusion (MATE) family. *Ann Bot* 106:199–203. <https://doi.org/10.1093/aob/mcq115>
- McClure BA, Hagen G, Brown CS, Gee MA, Guilfoyle TJ (1989) Transcription, organization, and sequence of an auxin-regulated gene cluster in soybean. *Plant Cell* 1:229–239
- McKenna A, Hanna M, Banks E, Sivachenko A, Cibulskis K, Kernytsky A, Garimella K, Altshuler D, Gabriel S, Daly M (2010) The genome analysis toolkit: a MapReduce framework for analyzing next-generation DNA sequencing data. *Genome Res* 20:1297–1303
- O'Brien TP, Feder N, McCully ME (1964) Polychromatic staining of plant cell walls by toluidine blue O. *Protoplasma* 59:368–373
- Pereira WE, Siqueira DL de, Puiatti M, Martínez CA, Salomão LCC, Cecon PR (2003) Growth of citrus rootstocks under aluminium stress in hydroponics. *Sci Agric* 60:31–41
- Rahman A, Bannigan A, Sulaman W, Pechter P, Blancaflor EB, Baskin TI, Division PB, Roberts S, Foundation N (2007) Auxin, actin and growth of the *Arabidopsis thaliana* primary root. *Plant J* 50:514–528. <https://doi.org/10.1111/j.1365-3113X.2007.3068.x>
- Rangel AF, Rao IM, Horst WJ (2009) Intracellular distribution and binding state of aluminum in root apices of two common bean (*Phaseolus vulgaris*) genotypes in relation to Al toxicity. *Physiol Plant* 135:162–173
- Ribeiro RV, Machado EC (2007) Some aspects of citrus ecophysiology in subtropical climates: re-visiting photosynthesis under natural conditions. *Braz J Plant Physiol* 19:393–411
- Ryan PR, Ditomaso JM, Kochian LV (1993) Aluminium toxicity in roots: an investigation of spatial sensitivity and the role of the root cap. *J Exp Bot* 44:437–446
- Ryan PR, Tyerman SD, Sasaki T, Furuichi T, Yamamoto Y, Zhang WH, Delhaize E (2011) The identification of aluminium-resistance genes provides opportunities for enhancing crop production on acid soils. *J Exp Bot* 62:9–20
- Santos CHdos, Hú GF, Rodrigues JD, Pinho SZ de (2000) Influence of different levels of aluminum on the development of citrus rootstock swingle citrumelo (*Citrus paradisi* mcf. x *Poncirus trifoliata* raf.) in nutrient solution. *Braz Arch Biol Technol* 43:0
- Sarruge JR, Haag HP (1974) Análises químicas em plantas. Escola Superior de Agricultura “Luiz de Queiroz”. Boletim Técnico, Piracicaba
- Sasaki T, Yamamoto Y, Ezaki B, Katsuhara M, Ahn SJ, Ryan PR, Delhaize E, Matsumoto H (2004) A wheat gene encoding an aluminium-activated malate transporter. *Plant J* 37:645–653. <https://doi.org/10.1111/j.1365-3113X.2003.01991.x>
- Schmohl N, Pilling J, Fisahn J, Horst WJ (2000) Pectin methylesterase modulates aluminium sensitivity in *Zea mays* and *Solanum tuberosum*. *Physiol Plant* 109:419–427. <https://doi.org/10.1034/j.1399-3054.2000.100408.x>
- Shaff JE, Schultz BA, Craft EJ, Clark RT, Kochian LV (2010) GEO-CHEM-EZ: a chemical speciation program with greater power and flexibility. *Plant Soil* 330:207–214
- Spartz AK, Ren H, Park MY, Grandt KN, Lee H, Murphy AS, Sussman MR, Overvoorde PJ, Gray WM (2014) SAUR inhibition of PP2C-D phosphatases activates plasma membrane H⁺-ATPases to promote cell expansion in *Arabidopsis*. *Plant Cell* 26:2129–2142. <https://doi.org/10.1105/tpc.114.126037>
- Stass A, Wang Y, Eticha D, Horst WJ (2006) Aluminium rhizotoxicity in maize grown in solutions with Al³⁺ or Al(OH)₄⁻—as predominant solution Al species. *J Exp Bot* 57:4033–4042
- Sun P, Tian Q, Chen J, Zhang W (2010) Aluminium-induced inhibition of root elongation in *Arabidopsis* is mediated by ethylene and auxin. *J Exp Bot* 61:347–356. <https://doi.org/10.1093/jxb/erp306>
- Swarup R, Perry P, Hagenbeek D, Van Der Straeten D, Beemster GTS, Sandberg G, Bhalerao R, Ljung K, Bennett MJ (2007) Ethylene upregulates auxin biosynthesis in *Arabidopsis* seedlings to enhance inhibition of root cell elongation. *Plant Cell* 19:2186–2196
- Tarazona S, García-Alcalde F, Dopazo J, Ferrer A, Conesa A (2011) Differential expression in RNA-seq: a matter of depth. *Genome Res* 21:2213–2223

- Von Uexküll HR, Mutert E (1995) Global extent, development and economic impact of acid soils. In: Date RA (ed) Plant Soil interactions at low pH. Kluwer Academic Publishers, Dordrecht, pp 5–19
- Wagner GP, Kin K, Lynch VJ (2012) Measurement of mRNA abundance using RNA-seq data: RPKM measure is inconsistent among samples. *Theor Biosci* 131:281–285
- Wang J, Chen D, Lei Y et al (2014) *Citrus sinensis* annotation project (CAP): a comprehension database for sweet orange genome. *PLoS ONE* 9:e87723
- Xu M, You J, Hou N, Zhang H, Chen G (2010) Mitochondrial enzymes and citrate transporter contribute to the aluminium-induced citrate secretion from soybean (*Glycine max*) roots. *Funct Plant Biol* 37:285–295
- Yang L-T, Jiang H-X, Tang N, Chen L-S (2011) Mechanisms of aluminum-tolerance in two species of citrus: secretion of organic acid anions and immobilization of aluminum by phosphorus in roots. *Plant Sci* 180:521–530
- Yang Z, Geng X, He C, Zhang F, Wang R, Horst WJ, Ding Z (2014) TAA1-regulated local auxin biosynthesis in the root-apex transition zone mediates the aluminum-induced inhibition of root growth in Arabidopsis. *Plant Cell* 26:2889–2904. <https://doi.org/10.1105/tpc.114.127993>
- Zhao Z, Feng JM, Kazuhiro M (2003) Differential Al resistance and citrate secretion in barley (*Hordeum vulgare* L.). *Planta* 139:794–800. <https://doi.org/10.1007/s00425-003-1043-2>
- Zhbannikov IY, Hunter SS, Foster JA, Settles ML (2017) SeqyClean: a pipeline for high-throughput sequence data preprocessing. In Proceedings of the 8th ACM International Conference on Bioinformatics, Computational Biology, and Health Informatics, pp 407–416. (ACM)
- Zhu XF, Sun Y, Zhang BC, Mansoori N, Wan JX, Liu Y, Wang ZW, Shi YZ, Zhou YH, Zheng SJ (2014) TRICHOME BIREFRINGENCE-LIKE27 affects aluminum sensitivity by modulating the O-acetylation of xyloglucan and aluminum-binding capacity in arabidopsis. *Plant Physiol* 166:181–189. <https://doi.org/10.1104/pp.114.243808>